Supporting Information

Yeh et al. 10.1073/pnas.1717489115

SI Materials and Methods

In Vitro Diapedesis Assay, Cell Culture, and Pharmacological Treatments. Human vascular umbilical endothelial vein cells (VECs) (purchased from Cell Application) were cultured on fibronectin (FN)-coated polyacrylamide (PA) gels for 48 h in medium M199 supplemented with 10% (vol/vol) endothelial cell growth medium (Cell Application), 10% (vol/vol) FBS (Lonza), 1% sodium pyruvate, 1% L-glutamine, and 1% penicillin–streptomycin (Gibco) until they formed a confluent monolayer. The HUVEC monolayers were treated with TNF-α (20 ng/mL) 24 h before the experiments to induce leukocyte recruitment. HL-60 cells (ATCC) were cultured in RPMI-1640 medium supplemented with 10% FBS and 1% penicillin–streptomycin. The HL-60 cells were then suspended in fresh medium at a concentration of 10^5/mL and treated with 1.25% (vol/vol) DMSO for differentiating into a neutrophil-like phenotype (1). Only the cells that had been differentiated for 4–6 d (dHL-60) were used in the experiments. Before performing the diapedesis experiments, TNF-α–treated VECs were further immersed in IL-1β (50 ng/mL) or N-formylmethionine-leucyl-phenylalanine (fMLP) (1 μM and 20 μM) for 2 h. After that, fresh-medium replacement was performed to establish a chemotactic gradient across the VEC monolayer. These treatments significantly increased the rate of diapedesis (Fig. S1). Additional diapedesis experiments were also performed by combining the fMLP treatments with either thrombin (1 U/mL) for 1 h or Y27632 (30 μM) for 30 min with thrombin stimulation. All chemical agents were then washed away and replaced with fresh medium for assessing the diapedesis phenomena. To elucidate the thrombin effect on VEC junctions, TNF-α–activated VECs were further treated with the thrombin for the indicated time points.

Three-Dimensional TFM. The 3D forces exerted by the cells on the substrate were measured using the 3DTFM methods previously reported by our group (2–4) (*SI Materials and Methods* and Fig. S2). We determined the 3D deformation of the substrate by imaging its top surface, which was seeded with fluorescent beads, using a confocal microscope. We used image correlation to determine two sets of substrate deformations relative to different reference states (i.e., the first recorded time point before diapedesis and a nondeformed, load-free reference state that was recorded after removing the cells by trypsinization). The first set of substrate deformations was used to calculate the temporal changes in the traction stresses at each of the stages during transmigration. The second set allowed us to determine the total absolute values of these traction stresses.

Three-Dimensional TFM Assay for Leukocyte Transendothelial Migration. We used a polyacrylamide gel assay and TFM to measure the 3D stresses generated by the endothelial cells and leukocytes during diapedesis (2–4). The experimental setup is summarized in Fig. S2. We fabricated 12-mm-diameter, 40-μm-thick PA gels of 5% acrylamide and 0.3% bisacrylamide [8.7 kPa (5)] on 35-mm glass-bottom dishes (FluoroDish) and seeded them with 0.03% carboxylate-modified microspheres (0.2-μm-diameter microbeads from Invitrogen). We mixed the acrylamide and bisacrylamide with 10% ammonium persulfate and tetramethylethylenediamine, placed a coverslip on top, and immediately inverted the mixture to let the gel polymerize for 30 min. During polymerization, the microspheres migrated to the bottom (i.e., the free surface of the gel). We used 0.15 mg/mL Sulfo-SANPAH (Thermo Fisher Scientific) followed by UV activation to facilitate the cross-linking of 50 μg/mL FN to the surface of the polyacrylamide gels. The gels were incubated overnight at 4 °C. We measured the thickness of the substrates by locating the top and bottom planes of the gel and subtracting their vertical positions as previously described (2).

We measured the 3D deformation of the substrate at its top surface by imaging the layer where the fluorescent microspheres were localized using a confocal microscope. We acquired time-lapse sequences of fluorescence z-stacks consisting of 17 planes separated 0.4 μm from each other at 2-min intervals. The 3D deformation was determined by cross-correlating each instantaneous z-stack with a reference z-stack. The z-stacks were divided into 3D interrogation boxes of $32 \times 32 \times 12$ pixels in the x, y, and z directions, respectively, to balance spatial resolution and signal-to-noise ratio. These settings provided a Nyquist spatial resolution of 2 μm in the three spatial directions.

We solved the elasticity equation of equilibrium for a linear, homogeneous, isotropic 3D body of Poisson's ratio $\sigma = 0.45$ (4),

$$(1-2\sigma)\nabla^2\boldsymbol{u} + \nabla(\nabla\cdot\boldsymbol{u}) = 0,$$

to determine the 3D deformation everywhere inside the substrate, $\boldsymbol{u}(x,y,z)$, from the 3D deformation measured on a single plane at the top of the substrate, $\boldsymbol{u}(x,y,h)$ (2, 3). In cell monolayers with gaps, we used Butler et al.'s (6) constrained iterative method to impose zero traction stresses at the surface of the substrate in the gaps. We applied Hooke's law to calculate the six independent components of the stress tensor everywhere inside the substrate. Particularly, we computed the 3D traction stress vector at the surface of the substrate in contact with the cells, $[\tau_{xz}(x,y,h), \tau_{yz}(x,y,h), \tau_{zz}(x,y,h)]$, and the horizontal and vertical axial stress inside the substrate, that is, $\tau_{xx}(x,y,z) + \tau_{yy}(x,y,z)$ and $\tau_{zz}(x,y,z)$, respectively.

Quantitative Endpoint Diapedesis Assay. Quantitative end-point diapedesis assays were performed as previously described (7). In brief, dHL-60 cells were resuspended in RPMI medium and stained with the green CMFDA dye (1 μM) for 30 min. After 30 min, dHL-60 cells were centrifuged to remove the staining solution and resuspended in a fresh M199 medium. The resuspended dHL-60 cells were then added to the confluent VEC monolayers (2×10^5 cells per well) in the upper chamber of a transwell (3-μm pore insert; Corning). fMLP (10 nM) was added in the lower chamber for generating the chemotactic gradient. Each transwell system was then kept at 37 °C for 1 h in a CO_2 incubator so diapedesis could take place. At the end of the incubation, VEC monolayers and dHL-60 cells were fixed in a freshly prepared 4% paraformaldehyde (pH 7.4) solution for 10 min. Before quantitative analysis, the VEC monolayers were stained with VE-Cadherin antibody and mounted onto glass slides for visualization (Vectashield mounting medium). Fluorescent images were taken under the Olympus IX81 confocal microscope with a cooled CCD (Hamamatsu). Diapedesis events were analyzed by counting at least 80 dHL-60 cells per condition and noting their position relative to the VEC monolayers. DHL-60 cells were defined as being above the VEC monolayer if more than 50% of their cell body was on or above the focal plane of the VEC nuclei. Otherwise, the cells were defined as being beneath the VEC monolayer.

Preparation of Anti-ICAM mAb-Coated Beads. Polystyrene beads (20 μm in diameter; Polyscience) were washed once with PBS and then treated with glutaraldehyde overnight at 4 °C for

cross-linking. After glutaraldehyde treatment, the beads were then combined with 200 μg/mL ICAM-1 mAb (G-5; Santa Cruz Biotechnologies) at room temperature with rotation for 6 h and washed by three times PBS. ICAM-1 mAb-coated beads were used immediately or stored at 4 °C for several days before use.

FITC–Dextran Permeability Assay. Confluent VECs were cultured in FN-treated six-well cell culture inserts (0.4-μm pore; Corning) for 48 h and treated with TNF-α overnight; 100 μg FITC-dextran (40 kDa; Sigma) in Hepes buffer was added to the upper chamber. Every 30 min, we collected samples (50 μL) from the lower chamber and replaced them immediately with the same volume of M199 medium to maintain hydrostatic equilibrium. We diluted the samples to 1 mL with PBS buffer, transferred 100 μL of each diluted sample into black 96-well black plates, and measured the fluorescent content at 492/520 nm absorption/emission wavelengths for FITC-dextran (Tecan).

Immunofluorescence and Confocal Microscopy. Cells were cultured on FN-coated substrates and stimulated as indicated. After treatments, cells were fixed in 4% (wt/vol) paraformaldehyde for 10 min. After fixation, cells were permeabilized in PBS supplemented with 0.1% (vol/vol) Triton X-100 for 10 min, followed by a blocking step in PBS supplemented with 5% (wt/vol) BSA. Cells were incubated with primary and secondary antibodies and after each step washed with PBS. DAPI was used for counterstaining. After mounting, z-stack image acquisition was performed on a confocal scanning microscope (Olympus IX81) with a cooled CCD (Hamamatsu), using Metamorph software (Molecular Devices) and a 40× N.A. 1.35 oil-immersion objective. Following the acquisition, the sequences of z-stack images were analyzed using Volocity software (PerkinElmer), which rendered the optical sections into 3D models, thus enabling analysis of leukocyte–VEC interaction dynamics. The remaining images were taken under an epifluorescence microscope, Olympus IX70.

Reagents. The antibodies against ICAM-1 and VE-Cadherin used in immunostaining were purchased from Santa Cruz Biotechnologies. The reagents of Alexa Fluor-488 Phalloidin, Cell Tracker green CMFDA dye, and Cell Mask deep red plasma membrane stain used for immunostaining and/or live cell labeling were purchased from Invitrogen. The carboxylate-modified red (580/605) microspheres used for 3DTFM were purchased from Invitrogen. TNF-α and IL-1β were purchased from R&D systems. fMLP and thrombin were purchased from Sigma-Aldrich. Y27632 was purchased from Abcam.

SI Results

Dynamics of VEC Cytoskeleton, Monolayer Gaps, and 3D Traction Stresses After Thrombin Treatment. Leukocyte transmigration is associated with an increase in vascular permeability, a pathophysiological consequence of inflammatory stimuli (8). To understand the dynamics of VEC junction integrity under acute inflammation we investigated the spatiotemporal changes of VEC cell–cell junctions and traction stresses following treatment with thrombin. Thrombin is an acute inflammatory mediator which modulates cell contractility via Rho activation, causing cell–cell junction remodeling and increased endothelial permeability (8).

We observed that the initial response to 1 U/mL thrombin treatment was a transient disruption of the VEC junctions leading to the formation of large intercellular gaps (Fig. S6). The remodeling of VEC junctions after thrombin treatment was accompanied by the appearance of actin stress fibers (Fig. S6*A*), suggesting that this process involved spatial and temporal changes in the contractile forces generated by the VECs. After 30 min, the gaps began to recede, so that their number remained elevated while their size diminished for the following 120 min (Fig. S6*B*). The permeability of the VECs, measured by the flux of 40-kDa FITC-dextran (Fig. S6*C*), increased significantly 30 min after thrombin treatment, and continued to increase 60–120 min posttreatment.

We measured the 3D traction stresses generated by the VECs at 30, 60, and 120 min after thrombin stimulation and stained their junctions (Fig. S6*D*). These measurements show that, 30 min after thrombin stimulation, there was an increase in both the in-plane and out-of-plane traction stresses localized at the edges of the newly formed monolayer gaps. The stress pattern observed during gap closure was markedly different from that observed in opening endothelial gaps during diapedesis (for comparison see Fig. 2*A*). The in-plane traction stresses were divergent from the monolayer edge, rather than convergent toward the gap, and there were both upward and downward stresses at the edge of the gap. As the gap closed the localized increase in traction stresses at the edge of the gap progressively disappeared.

1. Huveneers S, et al. (2012) Vinculin associates with endothelial VE-cadherin junctions to control force-dependent remodeling. *J Cell Biol* 196:641–652.
2. Del Alamo JC, et al. (2007) Spatio-temporal analysis of eukaryotic cell motility by improved force cytometry. *Proc Natl Acad Sci USA* 104:13343–13348.
3. del Álamo JC, et al. (2013) Three-dimensional quantification of cellular traction forces and mechanosensing of thin substrata by fourier traction force microscopy. *PLoS One* 8:e69850.
4. Álvarez-González B, et al. (2017) Two-layer elastographic 3-D traction force microscopy. *Sci Rep* 7:39315.
5. Tse JR, Engler AJ (2010) Preparation of hydrogel substrates with tunable mechanical properties. *Curr Protoc Cell Biol* Chapter 10:Unit 10.16.
6. Butler JP, Tolić-Nørrelykke IM, Fabry B, Fredberg JJ (2002) Traction fields, moments, and strain energy that cells exert on their surroundings. *Am J Physiol Cell Physiol* 282: C595–C605.
7. Muller WA, Weigl SA, Deng X, Phillips DM (1993) PECAM-1 is required for transendothelial migration of leukocytes. *J Exp Med* 178:449–460.
8. Reffay M, et al. (2014) Interplay of RhoA and mechanical forces in collective cell migration driven by leader cells. *Nat Cell Biol* 16:217–223.

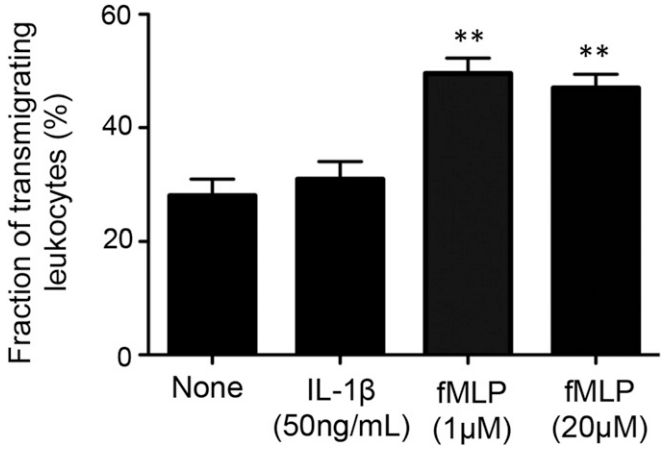

Fig. S1. Rate of leukocyte diapedesis as a function of chemotactic stimulus. Quantification of leukocyte diapedesis rates after 1 h of transmigration. The fraction of leukocytes that transmigrated was quantified as a function of the chemotactic stimuli on the VEC monolayers. Bars represent average fraction of transmigrated leukocytes. Data are expressed as mean ± SEM. $^{**}P < 0.01$. The data come from four independent experiments with more than 100 cells per group.

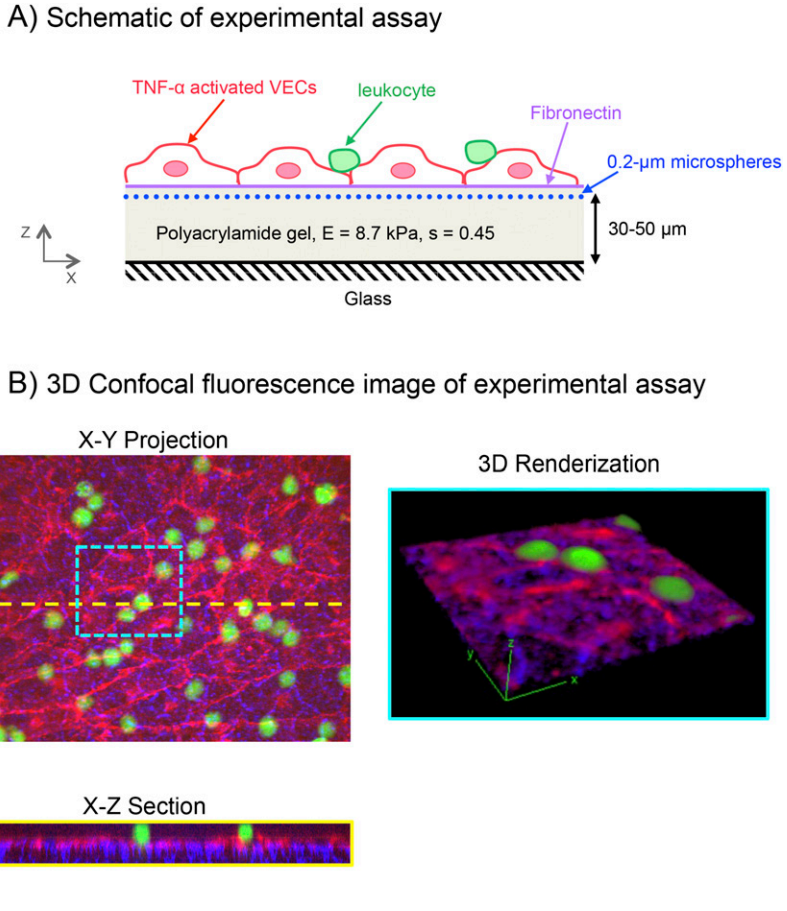

Fig. S2. Three-dimensional TFM assay for leukocyte transendothelial migration. (*A*) PA substrates with stiffness of 8.7 kPa seeded with fluorescent microspheres and coated with fibronectin were prepared as described in *SI Materials and Methods*. VECs were plated onto these gels and formed confluent monolayers. The VECs were treated with TNF-α to induce an inflammatory response for 24 h. To generate a chemotactic gradient for leukocyte diapedesis, the VEC monolayer was pretreated with IL-1β or fMLP as described in *SI Materials and Methods*. After removing the chemoattractants, dHL-60 cells were plated onto the VEC monolayer to map the spatiotemporal dynamics of the mechanical forces involved in the diapedesis process. Confocal z-stacks were recorded at 2-min intervals to record the motion of the fluorescent microspheres. At the end of each experiment, the cells were removed by trypsinization and a non-deformed, load-free reference state that was recorded. (*B*) The 3D confocal images for demonstraing the experimental assay.

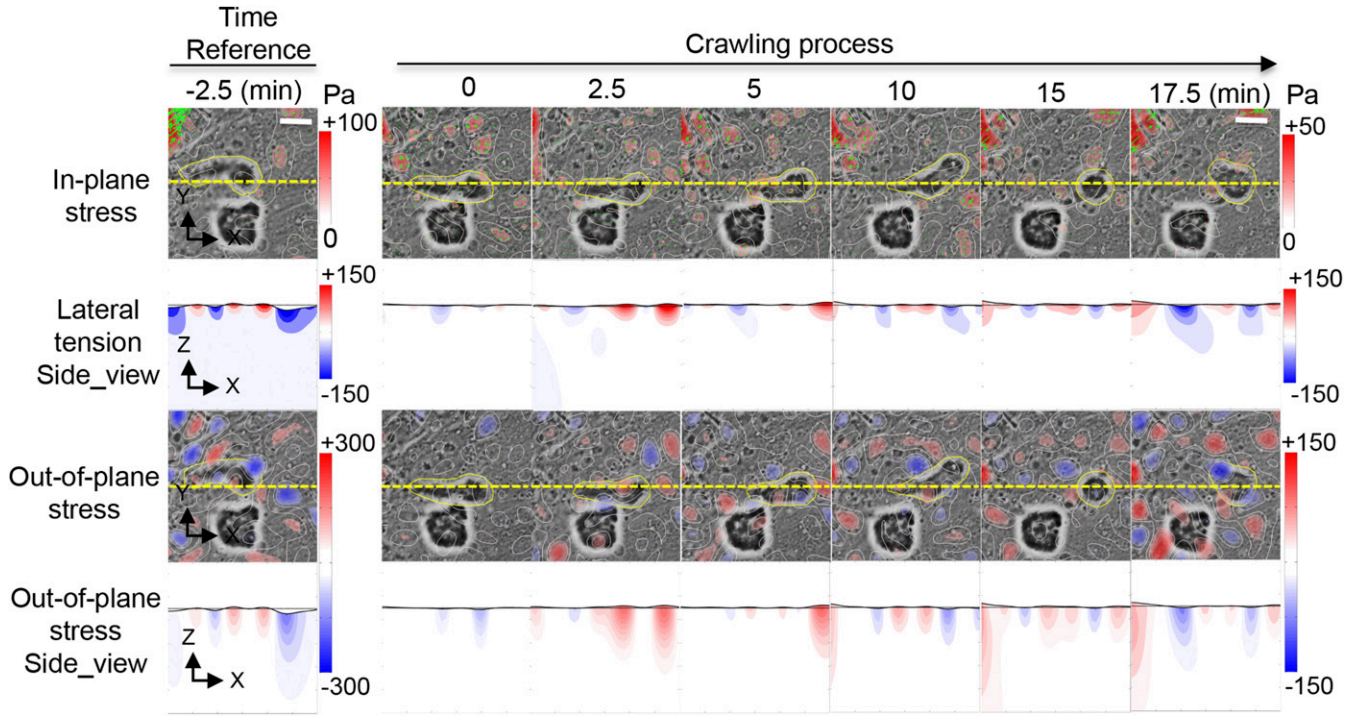

Fig. S3. Spatiotemporal evolution of the 3D stresses during leukocyte crawling over endothelial monolayers. Live-cell imaging of a leukocyte crawling over endothelial monolayers at indicated time points. The stress magnitude is given in pascals and represented by pseudocolor maps according to the color bars shown at the right-hand side of each panel sequence (row). The data are representative of leukocyte crawling events in three independent experiments. (Scale bar, 10 μm.)

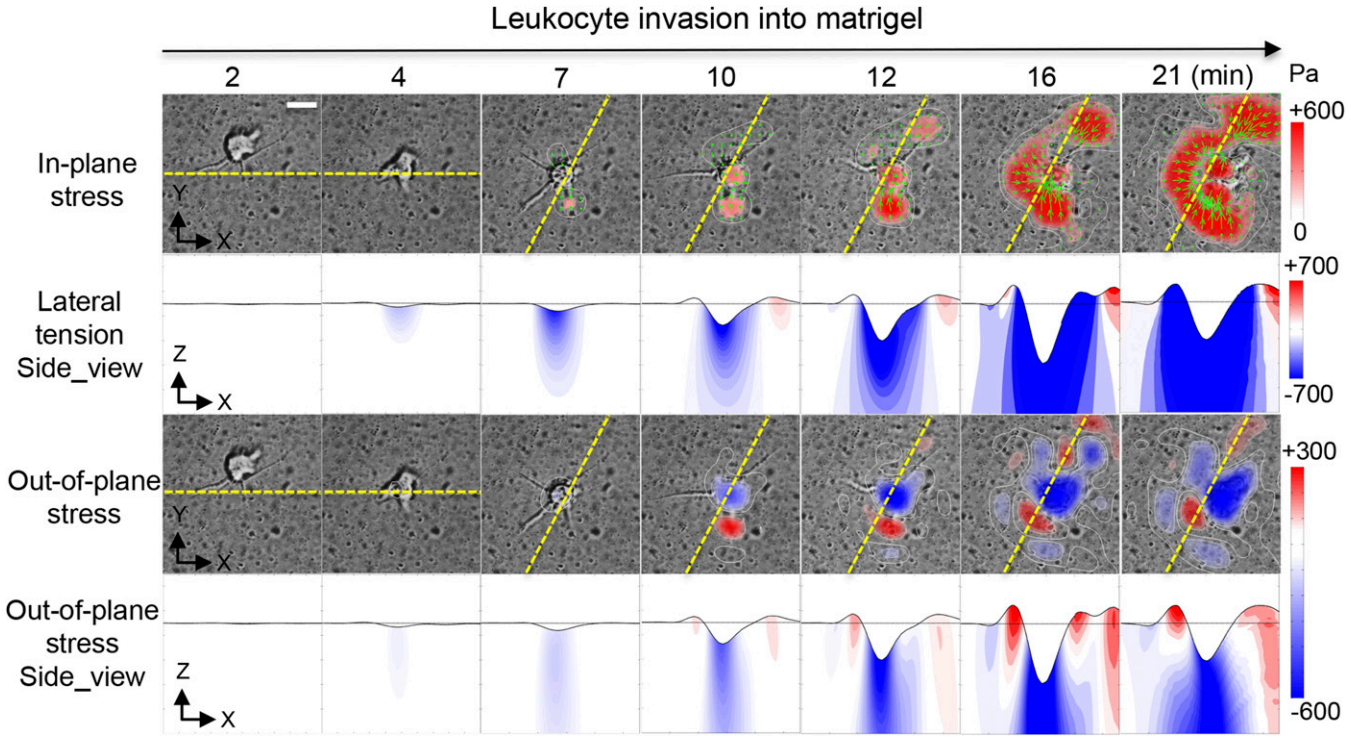

Fig. S4. Spatiotemporal evolution of the 3D stresses during leukocyte Invasion into Matrigel. Live-cell imaging of a leukocyte invasion into Matrigel at indicated time points. The stress magnitude is given in pascals and represented by pseudocolor maps according to the color bars shown at the right-hand side of each panel sequence (row). The data are representative of leukocyte invasion events in three independent experiments. (Scale bar, 10 μm.)

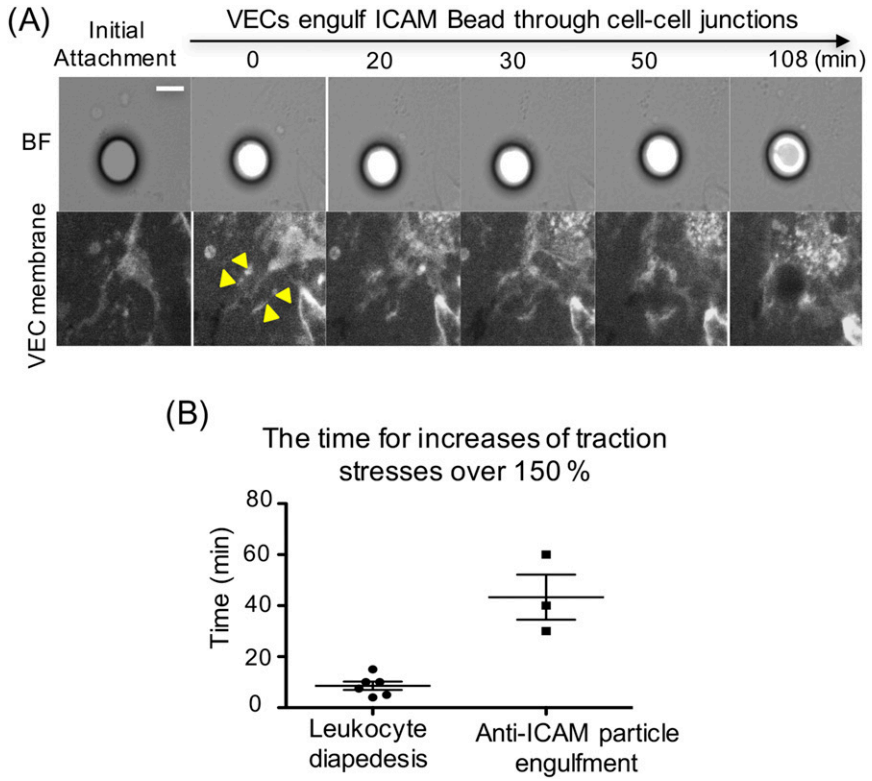

Fig. S5. The dynamics of anti-ICAM bead engulfment by VECs at cell–cell junctions. (*A*) Epifluorescent live-cell imaging of VEC junctions stained by CY5 cell membrane dye shows an anti-ICAM-coated bead being engulfed by the VEC junctions. Yellow arrows indicate the endothelial membranes, which bind to the anti-ICAM-coated bead. The images are representative of anti-ICAM bead inclusion events in three independent experiments. (Scale bar, 10 μm.) (*B*) The time taken for the traction stresses to rise by over 150% in leukocyte diapedesis and anti-ICAM bead engulfment cases.

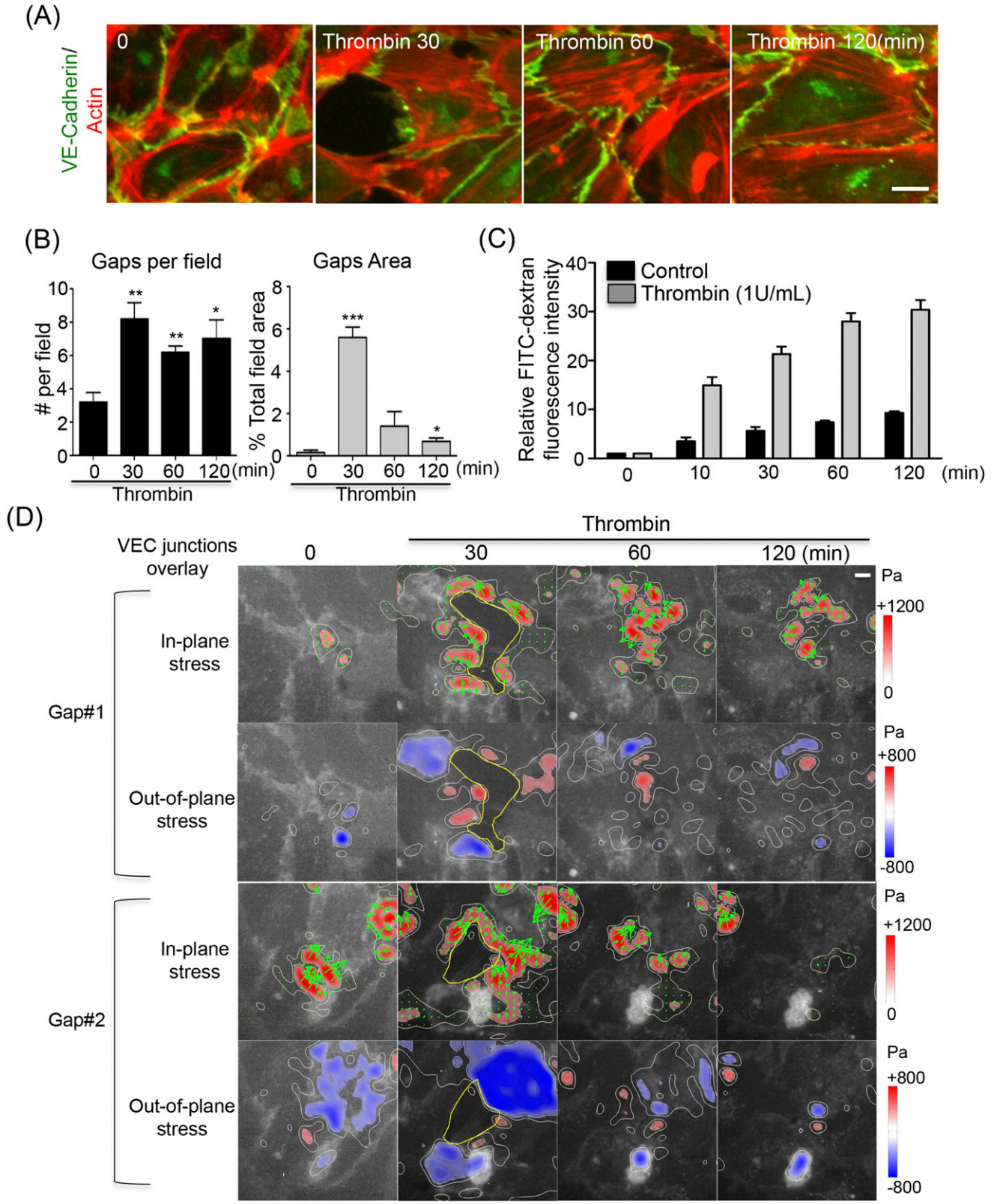

Fig. S6. Dynamics of the VEC cytoskeleton, monolayer gaps, and 3D traction stresses after thrombin treatment. (*A*) Merged fluorescent images of VECs stained for VE-Cadherin (green) together with F-actin (red). (Scale bar, 10 μm.) (*B*) Quantification of the number of gaps per field and the percentage of total gap area per field in thrombin-treated VECs. (*C*) FITC-dextran permeability across a VEC monolayer is measured with a transwell, two-compartment system. Samples were taken from the lower compartment at indicated time points. The results are plotted as normalized FITC-dextran concentrations. (*D*) Spatiotemporal dynamics of VEC junction remodeling and traction stresses after 30 min of thrombin treatment. The maps show representative spatial distributions of in-plane traction stresses (second column) and out-of-plane traction stresses (third column). The level of stresses in pascals is represented by a pseudocolor map according to the color bars shown at the right-hand side of the figures. (Scale bar, 10 μm.) The data shown in this figure are representative of at least three independent experiments.

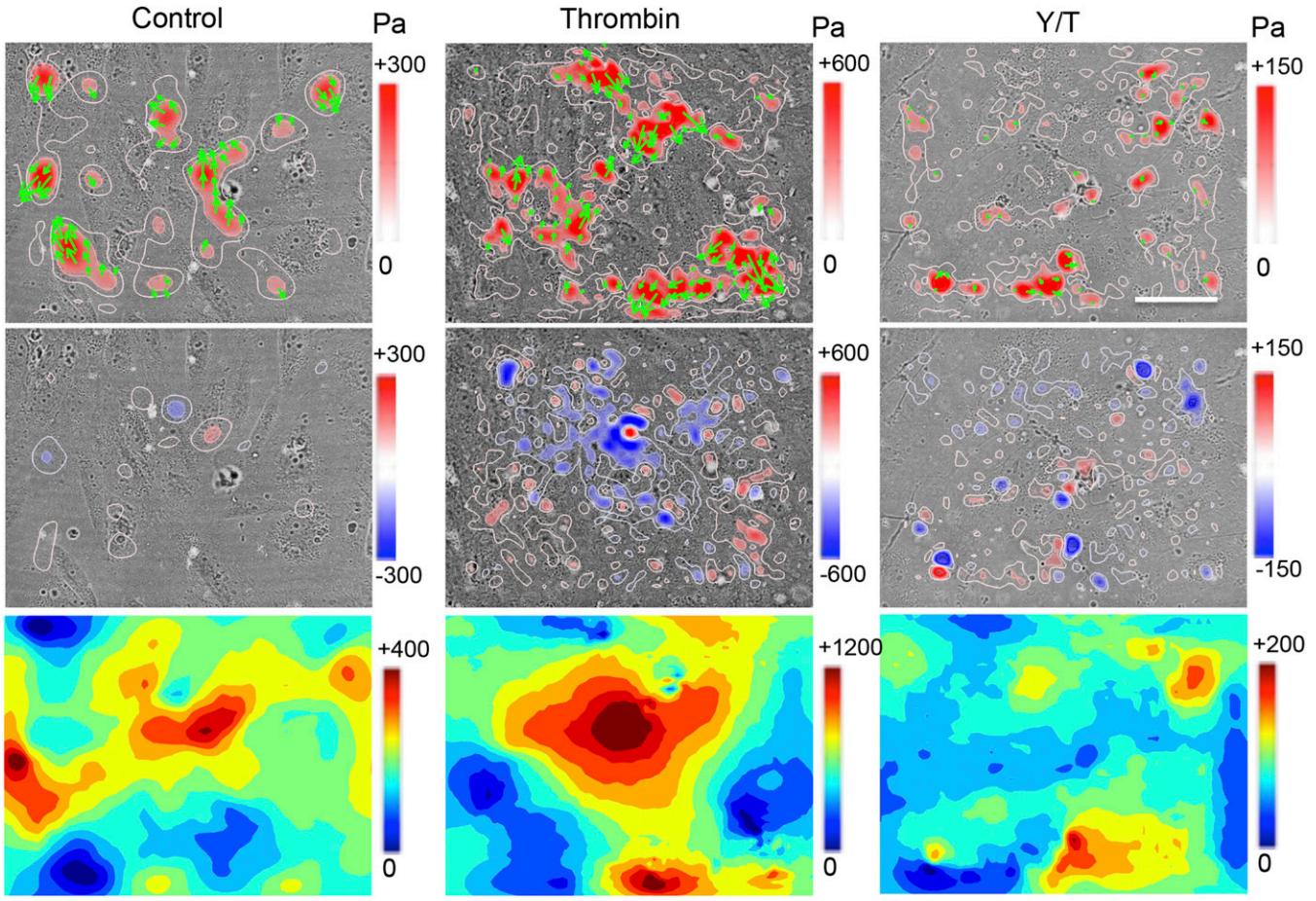

Fig. S7. Thrombin treatment increases heterogeneity in the distribution of mechanical tension within the VEC monolayer. Three-dimensional traction stresses and mechanical tension within the monolayer. Maps showing representative spatial distributions of in-plane traction stresses (first column) and out-of-plane traction stresses (second column) and monolayer tension (third column). Note that the tension fluctuations have higher magnitude in the thrombin-treated case as indicated by the color bars. The images are representative of three independent experiments. (Scale bar, 50 μm.)

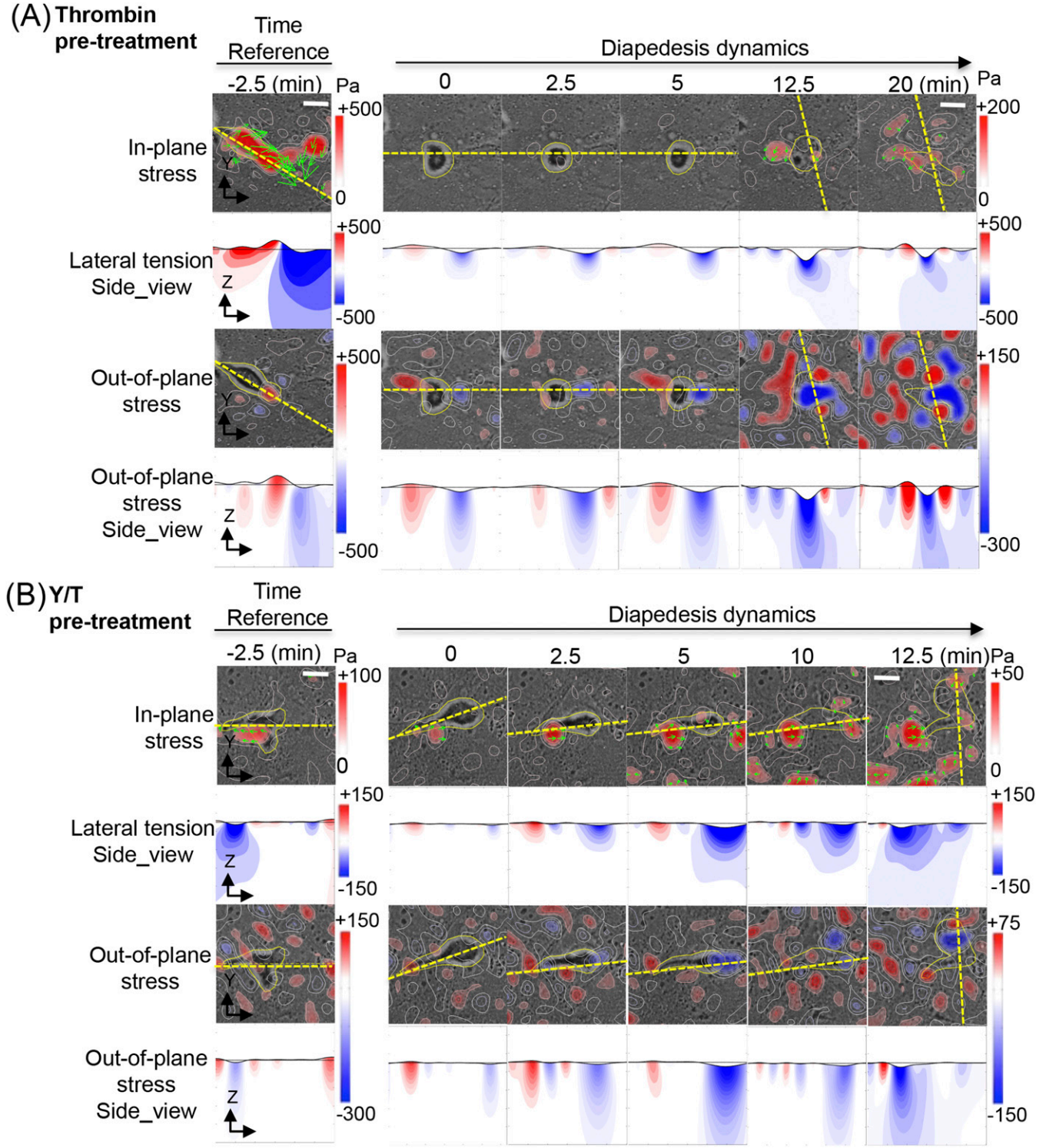

Fig. S8. Spatiotemporal evolution of the 3D stresses during diapedesis across monolayers treated with thrombin and thrombin plus Rho kinase inhibitor. Live-cell images of a leukocyte crawling, firmly adhered, and transmigrating across VEC monolayers pretreated with thrombin (*A*) and thrombin+Y-27632 (*B*). The stress magnitude is given in pascals and represented by pseudocolor maps according to the color bars shown at the right-hand side of each panel sequence (row). Similar to Fig. 2, rows 1 and 3 represent respectively the in-plane traction stress (τ_{xz} and τ_{yz}) and the out-of-plane traction stress (τ_{zz}) overlaid on bright-field cell images. Likewise, rows 2 and 4 represent respectively the tension ($\tau_{xx}+\tau_{yy}$) and the vertical stress (τ_{zz}) of the matrix in an XZ plane section that intersects the endothelial monolayer along the yellow dashed line shown in rows 1 and 3. The images are representative of at least five independent experiments. (Scale bars, 10 μm.)

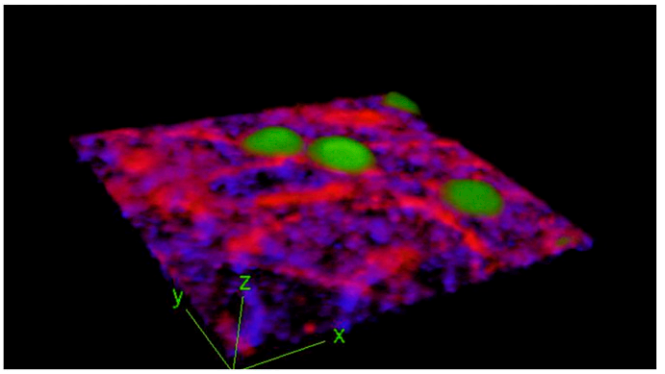

Movie S1. Movie for 3D confocal images of experimental setup.

Movie S1